# Imaging Bolometers for Visualization of Plasma Radiation and Cross-Validation of Three Dimensional Impurity Transport Models for the Large Helical Device*)

Byron J. PETERSON, Evgeny A. DRAPIKO[1)], Kiyofumi MUKAI, Masahiro KOBAYASHI, Shwetang N. PANDYA[2)], Ryuichi SANO[2)] and the LHD Experiment Group

*National Institute for Fusion Science, 322-6 Oroshi-cho, Toki 509-5292, Japan*
[1)]*Kurchatov Institute, Moskow 123182, Russia*
[2)]*Graduate University for Advanced Studies, 322-6 Oroshi-cho, Toki 509-5292, Japan*

(Received 7 December 2012 / Accepted 8 March 2013)

The InfraRed imaging Video Bolometer (IRVB) measures the radiation from the plasma in two dimensions, giving an image of the plasma radiation power loss. Using a geometry matrix calculated from a model of the LHD first wall, the IRVB sightline geometry and a three dimensional (3D) plasma grid, a synthetic instrument is developed using the 3D carbon impurity radiation results of the EMC3-EIRENE edge impurity transport code as an input. The output of the synthetic instrument are images of the plasma radiation at the IRVB foil due to the EMC3-EIRENE code, which are qualitatively compared with preliminary experimental images from the IRVB. Such a comparison for detached discharges in LHD in which an externally induced $m/n = 1/1$ magnetic island is applied shows that when the magnetic island is moved 36 degrees toroidally the enhanced radiation in the x-points of the magnetic island also moves as predicted by the EMC3-EIRENE code.



Keywords: bolometer, imaging, plasma radiation, LHD, synthetic instrument

DOI: 10.1585/pfr.8.2402037

## 1. Introduction

Bolometry is the measurement of total radiated power from the plasma of fusion devices. Traditional resistive bolometers [1] consist of a thin foil, which absorbs the radiation from the plasma. The energy from the radiation absorbed by the foil is transferred through an isolation layer to a thin metal meander, which serves as a temperature sensitive resistor. Electrical measurement of the change in resistance gives a measure of the absorbed radiation. These detectors are typically arranged in one dimensional arrays around one poloidal cross-section of the device and the signals are analyzed using a tomographic inversion to produce a two dimensional (2D) profile of the plasma radiation. This is usually sufficient in a tokamak geometry, where the toroidal dimension can be ignored, but in a three dimensional (3D) geometry, such as that present in the Large Helical Device (LHD), a 3D measurement is called for. In addition, resistive bolometers have not yet demonstrated that they can survive in the harsh high temperature, high neutron flux environment of a fusion reactor. These two issues have driven the development of a new type of bolometer diagnostic at the National Institute for Fusion Science known as the InfraRed imaging Video Bolometer (IRVB) [2, 3]. This device also relies on a thin foil, albeit one that is suspended in a copper frame. The front side of the foil views the plasma through an aperture, forming a pinhole camera, while the back side of the foil is blackened with graphite to strongly emit the absorbed radiation from the plasma in the infrared (IR). This IR radiation is detected by an IR camera located outside the vacuum vessel, which views the foil through appropriate IR optics and an IR vacuum window and measures the change in the foil temperature due to the absorbed plasma radiation. By solving the 2D heat diffusion equation on the foil a 2D measurement of the radiation absorbed by the foil is derived and utilizing the pinhole camera a 2D image of the plasma radiation is obtained. This image of the plasma radiation can be used in two ways. The ultimate goal of this research on LHD is to operate multiple IRVBs on LHD and perform 3D tomography to provide a 3D measurement of the plasma radiation, which can be compared with the 3D carbon radiation results from the EMC3/Eirene [4, 5] 3D edge impurity transport code. This requires the calculation of a geometry (transform) matrix for each IRVB, which relates the plasma radiation emitted by each element of a 3D plasma grid to the signal measured by each bolometer pixel on the foil. This calculation depends on the geometry of the pinhole camera, the geometry of the LHD first wall and the geometry of the predefined plasma grid. As long as the plasma grid does not depend on any plasma parameters such as magnetic flux surfaces, the geometry

*author's e-mail: peterson@LHD.nifs.ac.jp*
*) This article is based on the presentation at the 22nd International Toki Conference (ITC22).

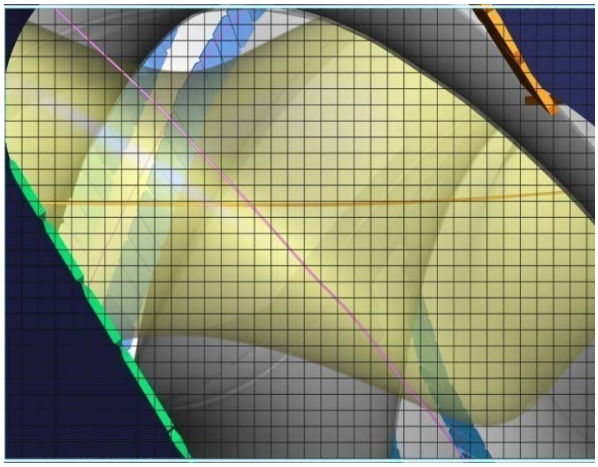

Fig. 1 Computer aided drawings of FoVs for IRVB at Port 10-O. Pink lines show traces of helical divertor x-points.

matrix is independent of the plasma and only needs to be calculated once for each IRVB. Recently four IRVBs are operating on LHD, but much calibration work remains to be done before such a tomographic inversion can be attempted. The second technique is to use a synthetic instrument, which transforms the 3D carbon radiation results from the EMC3/Eirene code using the geometry matrix to the resulting radiation at the IRVB foil from the code result. Then this can be directly compared to the radiated power image from the IRVB without performing the tomographic inversion. In this paper we briefly introduce the IRVB in Section 2, explain the calculation of the geometry matrix and the synthetic images in Section 3 and then present the comparison of the synthetic images and the IRVB images in Section 4. Finally, a summary will be given in Section 5.

## 2. InfraRed Imaging Video Bolometers

In this paper the results from one IRVB on LHD are shown. LHD has a ten-fold periodic symmetry in the toroidal direction. Each of the 10 field periods that make up the device are numbered 1 – 10. This IRVB views the plasma semi-tangentially from port 10-O (O indicates an outer port on the equatorial midplane of the device) using a Phoenix/FLIR IR camera [6]. The IRVB uses a 9 cm × 7 cm × 2-4 micron Pt foil viewing the plasma through a 4 mm × 4 mm square aperture. The number of IRVB channels is 32 × 24 and the time resolution is approximately 4.4 ms (225 frames per second). The field of view (FoV) for the IRVBis shown in Fig. 1.

## 3. Calculation of Geometry Matrices and Synthetic Images

For each IRVB a geometry matrix, $T_{ij}$, is calculated which quantifies the contribution of the radiation from each plasma sub-volume, $S_j$, to each bolometer detector's signal, $P_i$, as expressed in Eq. (1).

$$P_i = \sum_j \frac{\Omega_{ij}}{4\pi} V_{ij} S_j = \sum_j T_{ij} S_j. \quad (1)$$

The geometry matrix has the plasma sub-volume index, $j$, as one dimension and the detector index, $i$, as another dimension. The cylindrical plasma grid used for the geometry matrix calculation has the dimensions of 5 cm major radially (2.5 m < $R$ < 5.0 m, 50 divisions), 5 cm vertically (−1.3 m < $Z$ < 1.3 m, 52 divisions) and one degree in toroidal angle, $\phi$, (180 divisions for the half torus where the IRVBs are located). The total number of plasma elements is then 468,000. This covers the core plasma and ergodic edge, but not the divertor region. The geometry matrices are calculated by subdividing the FoVs of each detector pixel into sub-volumes having a maximum dimension of 1 cm. For each sub-volume the volume, $V_{ij}$, is calculated and weighted by the solid angle, $\Omega_{ij}$, represented by the bolometer pixel at the sub-volume and then added to the appropriate element of the geometry matrix corresponding to the detector number, $i$, and the plasma subvolume, $j$, in which the center of the FoV sub-volume is found. A model of the LHD first wall is used to stop the calculation when the FoV sub-volume intersects the wall.

The EMC3/Eirene code calculates the 3D carbon radiation distribution in the LHD edge plasma in a very fine (1-2 mm) irregularly spaced grid in $R$ and $Z$ and 1 degree spacing in $\phi$. This is resampled into the same 5 cm × 5 cm × 1° grid of the geometry matrix. The synthetic images are then generated by multiplying the geometry matrix for the IRVB, $T_{ij}$, by the 3D carbon radiation, $S_j$, from the EMC3/Eirene calculation, as indicated in Eq. (1).

## 4. Comparison of Synthetic Images and IRVB Data

As an example of a comparison between the EMC3/Eirene-based synthetic images and the IRVB images, data is taken from discharges in which an $m/n = 1/1$ magnetic island (where $m$ and $n$ are the indicies of the poloidal and toroidal harmonics, respectively) is used to break the $m = 2$, $n = 10$ symmetry of the LHD magnetic field and induce and stabilize a detached plasma [7–9]. In these discharges it has been observed that during the detachment with the magnetic island the radiation is localized in the x-point of the magnetic island which is toroidally localized and centered on the inboard side at the same field period as the o-point which is centered on the outboard side. In Fig. 2 synthetic images from the EMC3/Eirene code (a), (b), (c) and corresponding IRVB data (d), (e), (f), from three time frames are shown. Figures 2 (a) and (d) show the radiation from an attached plasma. The radiation pattern along the helical divertor x-points (which have the $m = 2$, $n = 10$ helical symmetry and are indicated by light blue lines) shown in the synthetic image is also seen in the

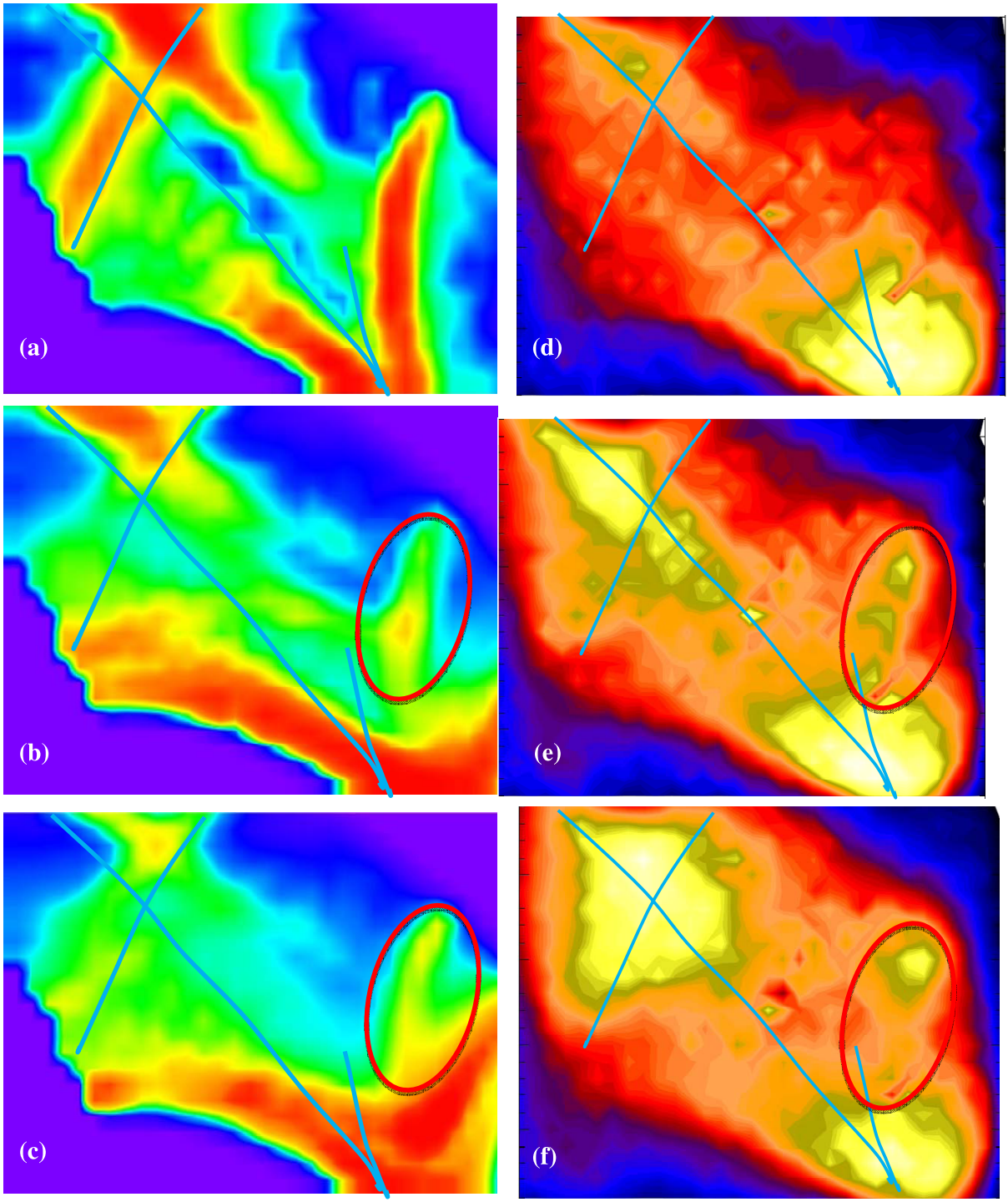


Fig. 2 Synthetic images of carbon radiation from the edge plasma from EMC3/Eirene code at port 10-O IRVB for (a) attached plasma and detached plasma with magnetic island at (b) 6-O port and at (c) 7-O port. Corresponding IRVB images from 10-O port for shot 99174 at (d) 4.3 s, (e) 4.9 s, and (f) shot 99186 at 5.0 s. Light blue lines indicate helical divertor x-point traces. Red ovals indicate region of radiation from magnetic island x-point. Note that the color scheme is different for the synthetic images and IRVB data to emphasize a qualitative comparison.

IRVB data, but not as clearly pronounced. Next, radiation images are shown from detached plasmas with the o-point of the magnetic island centered at the 6-O port in images (b) and (e) and at the 7-O port in images (c) and (f). The region with radiation from the x-point of the magnetic island is indicated with a red oval. Upward motion of the radiation pattern with the motion of the magnetic island is seen in both the synthetic and IRVB images. Also there are some notable discrepancies between the synthetic images and the IRVB data. In particular, where the x-point traces cross each other in the FoV of the IRVB in the upper right hand corner, there is a bright point in the IRVB data which

does not appear in the model. After the calibration data is included in the analysis then it will be clear to what extent the model does or does not agree with the experimental data.

# 5. Summary

In this paper preliminary radiation images from an IRVB on LHD are qualitatively compared with synthetic images derived from the EMC3/Eirene edge impurity transport code. Details of the radiation from the helical divertor x-points seen in the synthetic image are reflected in the experimental results. Motion of the radiation localization point as the O-point of the magnetic island is moved from port 6-0 to 7-O is also observed. However, this comparison is not conclusive since there are also major disagreements between the experimental data and the model and it is not clear whether this is due to improper modeling or due to some non-uniformities in the IRVB foil thermal characteristics that have not yet been corrected through calibration. Future work includes completing the calibration analysis and integration into the IRVB image analysis to give an absolutely calibrated IRVB image that can be quantitatively compared with the synthetic image. Then the code impurity transport parameters can be modified to match the experimental results to give a more accurate understanding of the impurity transport.

# Acknowledgement

This work is supported by NIFS administrative grants NIFS12ULHH026, NIFSGGHH001, NIFSGGHH003 and NIFSGGHH004.

[1] K.F. Mast *et al.*, Rev. Sci. Instrum. **62**, 744 (1991).
[2] B.J. Peterson, Rev. Sci. Instrum. **71**, 3696 (2000).
[3] B.J. Peterson *et al.*, Rev. Sci. Instrum. **74**, 2040 (2003).
[4] Y. Feng *et al.*, Contrib. Plasma Phys. **44**, 57 (2004).
[5] D. Reiter *et al.*, Fusion Sci. Technol. **47**, 172 (2005).
[6] www.flir.com
[7] M. Kobayashi *et al.*, Phys. Plasmas **17**, 056111 (2010).
[8] B.J. Peterson *et al.*, J. Nucl. Mater. **415**, S1147 (2011).
[9] E.A. Drapiko *et al.*, Nucl. Fusion **51**, 073005 (2011).